Title page

Article Title: A virtual reality collaborative planning simulator and its method for three machines in a fully mechanized coal-mining face

Authors: XIE Jiacheng[a]，YANG Zhaojian[a]，WANG Xuewen[a]，Zeng Quanren[b]，LI Juanli[a]，LI Bo[a]

Author affiliations:

a. College of Mechanical Engineering, Key Laboratory of Fully Mechanized Coal Mining Equipment, Taiyuan University of Technology, Shanxi 030024,China;

b. Department of Design, Manufacture and Engineering Management, University of Strathclyde, Glasgow, UK

Corresponding author name: YANG Zhao-jian

Affiliation:

College of Mechanical Engineering, Key Laboratory of Fully Mechanized Coal Mining Equipment, Taiyuan University of Technology, Shanxi 030024,China

Detailed permanent address:

No.216 mailbox, HuYu Campus, Taiyuan University of Technology, No.18, Xin KuangYuan Road, TaiYuan, ShanXi Province, P. R. China

Email address:yangzhaojian@tyut.edu.cn;tyutyangzhaojian@163.com

Telephone number:86-15333014310;86-03516010414

Acknowledgements

This work is supported by Shanxi Postgraduate Education Innovation Project(No. 2017BY046), Shanxi Scholarship Council of China(No.2016-043), Program for the Outstanding Innovative Teams of Higher Learning Institutions of Shanxi (No.2014), Shanxi Province Scholars Scientific and Technological Activities Preferred Funding Project (No.2016) and Applied Basic Research Project of Shanxi(No.201601D011050).

A virtual reality collaborative planning simulator and its method for three machines in a fully mechanized coal-mining face

Abstract: The existing automatic control program and its parameters for three machines in a fully mechanized coalmining face are static and simplex and are therefore inadequate for satisfying the complex and dynamic environment of underground coal mines. To overcome this problem, a collaborative mathematical model is established that includes the effects of a dynamic environment. A virtual reality collaborative planning simulator with methods for the three machines is also proposed based on a multi-agent system (MAS). According to the dynamic characteristics of the environment, equipment and technologies, a fully mechanized Unity3D simulator (FMUnitySim) is designed in terms of multiple factors and multiple dimensions. The factors affecting the coordinated operation of the three machines are analyzed and modeled. The communication modes, coordination, and redundant sensing process among multiple agents, which include the shearer agent and the scraper conveyor agent, are also investigated in detail. Using this system, the key parameters of the three machines can be planned and adjusted online to design and distinctly observe the corresponding collaborative simulations of coordinated operation with multiple perspectives and in real time. Tests of different maximum shearer haulage speeds for regular or reverse transporting coal are designed; their key parameters, including the average shearer haulage speed, average follower distance, and average scraper conveyor load, are planned and simulated using FMUnitySim. The optimal parameter combination is obtained by analyzing and comparing the simulation results. The proposed FMUnitySim offers an effective means and theoretical basis for the rapid planning and safe automatic production of a fully mechanized coalmining face.

Keywords: Three machines in a fully mechanized coal-mining face; Virtual planning; Collaborative mathematical model; Multi-agent system; Parameter matching; Unity3D

List of symbols

A_{area}	Maximum cross-sectional area to transport coal for the scraper conveyor
$A(t)$	Cross-sectional area to transport coal for the scraper conveyor at moment t
B_{normal}	Critical value of the roof broken degree
$B_{zj}(i)$	Corresponding roof broken degree of hydraulic support No. i
D_{drum}	Drum diameter of the shearer
D_{follow}	Follower distance
D_{zbc}	Middle trough width of the scraper conveyor
f_1	Running resistance coefficient of the scraper chain
f_2	Running resistance coefficient of coal
$f(S_r(t))$	Cutting height of the rear drum at the position of $S_r(t)$
H_c	Machine height of the shearer
H_{down}	Length of the retracting columns
H_{rise}	Length of the rising columns
$H_u(i)$	Corresponding mine height of middle trough No. i
$H_{zj}(m)$	Height of hydraulic support No. m
I_{motor}	Virtual electric current of the virtual shearer
J	Cutting depth of the shearer
K_g	Capacity decline coefficient of the scarper conveyor due to poor operating conditions
L	Length of the working face (m)
l	Distance of the cutting position and unloading position
L_{gbj}	Running distance of the shearer from moment t_1 *to* moment t_2
L_{JiTou}	Distance from the front drum to the unloading point of the shearer
L_{JiShen}	Distance from the left drum hinge point to the right drum hinge point for the shearer
L_{wan}	Distance from the start point of the shearer to the coal seam

L_y	Length of the shearer rocker arm
$m_{front}(t)$	Cutting amount of the front drum from the beginning to moment t
$m_{Ins-front}(t)$	Instantaneous coal cutting amount of the front drum at moment t
$m_{Ins-rear}(t)$	Instantaneous coal cutting amount of the rear drum at moment t
$m_{Ins-transport}(t$	Instantaneous amount of shipped coal
$m_{rear}(t)$	Coal cutting amount of the rear drum from the beginning to moment t
$m_{total-transpor}$	Total cutting amount of the shearer from the beginning to moment t
m_{sudd}	Mutation load of the scraper conveyor caused by the collapse of the coal wall
N	Serial number of the advancing hydraulic support
n_{broken}	Influence parameter of the broken roof
$n_{condition}$	Influence parameter of the equipment working condition
n_{hy}	Influence parameter of the action mode
n_{press}	Influence parameter of the mine pressure
N_{motor}	Motor load of the scraper conveyor
P_{normal}	Critical value of the roof pressure for the hydraulic support
$P_{zj}(i)$	Corresponding roof pressure value of hydraulic support No. i
Q_{permit}	Maximum permitted power of transporting coal
q_0	Scraper chain weight per meter (kg/m)
$q(t)$	Mine stream amount of the current middle trough per meter
$Q(t)$	Total load of the scraper conveyor from the beginning to moment t
$Q_{Ins}(t)$	Scraper conveyor load at moment t
$S(t)$	Shearer fuselage position at moment t
$S_f(t)$	Front drum position at moment t
$S_r(t)$	Rear drum position at moment t
$S_{zj}(m)$	Position of hydraulic support No. m
$S_{tuiyi}(m)$	Elongation length of the advancing units for hydraulic support No. m
S_{r-l}	Action area of the columns
S_{d-l}	Action area of the advancing units
$state(m)$	State of hydraulic support No. m
t_0	Running start moment of the shearer
t_1	Moment when the front drum begins to cut coal
t_2	Moment when the scraper conveyor begins to transport coal shipped out
t_3	Moment when the rear drum begins to cut coal
$t_{norm-move}$	Action time of the hydraulic support
V_o	Relative speed from V_c *to* V_g
V_g	Scraper conveyor chain speed
V_c	Shearer haulage speed
V_y	Advancing speed of the hydraulic support
YiJiaFa-ngShi	Current advancing mode of the hydraulic support
X(i)	Corresponding X coordinate of middle trough No. i
η	Transmission mechanism efficiency of the scraper conveyor
β	Dip degree of the coal seam (degrees)
$\alpha_{S(t)}$	Relative angle of the front drum to the fuselage at the position of *S (t)*
$\alpha_{rS(t)}$	Relative angle of the rear drum to the fuselage at the position of *S (t)*
ρ_{soild}	Density of solid coal
$\rho_{dispersion}$	Density of bulk coal
λ	Divisor of (*Sr*(*t*)- *Sr*(*t3*))/Dzbc
σ	Remainder of (*Sr*(*t*)- *Sr*(*t3*)) %Dzbc
$\phi(m)$	Flap angle of hydraulic support No. m

1. Introduction

With the advent of "Industrial 4.0" and "Internet Plus", fully mechanized mining equipment has developed from the traditional manual control stage to the electro-hydraulic control stage with hydraulic support and finally to the intelligent collaborative control stage[1]. In certain well-conditioned coal mines, fully mechanized mining equipment with intelligent collaborative control has been shown to reduce the labor intensity of coal miners and to improve the efficiency of coal production[2]. However, because of the static and simplex nature of

setting parameters in the existing collaborative control program of the three machines, intelligent collaborative control, which is prone to unknown problems, cannot adapt to the complex environment and become the main production mode of coal mining [3].

To improve this situation, the three machines must be adaptive to the dynamic environment and have a “life form”, which includes abilities such as self-perception, self-decision and self-adaptation. Based on this concept, several scholars have introduced the idea of "mining robots", which is considered the mainstream research direction for unmanned coal mining [4-5]. With the introduction of a multi-agent system (MAS) to the field of three machines in a fully mechanized coalmining face, Fan established the three-machine task planning model and simulated a three-machine operation with the Generalized Partial Global Planning(GPGP) theory. However, Fan did not achieve the expected results because of the singularity of the model and his assumptions of an ideal environment [6].A complex and reliable mathematical model that can portray real-life situations is the basis of simulation and planning. However, the current main stream planning and simulation process is too abstract for general engineering personnel to implement. If the simulation process is visualized and the whole planning process is displayed in a more realistic manner, then the software’s versatility and digital design ability will be greatly improved.

Virtual reality (VR) technology has been rapidly developing in recent years and, if combined with planning technology, shows great potential for visualizing the entire planning process. Widely used VR software for planning include OpenGL, Unreal, and Unity3D. These software programs are used to construct 3D simulation environments, such as OpenSim [7], V-REP [8], Delta3D [9], USARDim [10] and Gazebo [11]. Among them, Unity3D has received particular attention because of its advantages in visual interface, multi-platform release, and shielding of its underlying code. With Unity3D, WonsilLee [12] created a simulation of a room with Internet of Things (IoT), where virtual sensors were added to simulate the interaction between people and the indoor environment. The MAS theory was used in another application of Unity3D. Christian Hu [13] established a 3D visualization environment of an airplane cabin that simulates and visualizes the passengers’ behavior awareness and path. By establishing a real-time 3D multi-aircraft path planning and simulation system [14-15], a proposal was put forward to couple the virtual environment with actual sensors, such as radars. This simulation system can visually control the aircraft and verify the algorithm of path planning. Xu Z. et al. [16] and Cha et al. [17] established a VR fire training simulator. Mancal et al. [18] established an accident simulation to train process-industry operators in a virtual environment. These VR planning simulators have achieved very good results and have contributed to the development of many industries.

VR technology has been widely used in the coal mining field because of its intuitive, immersive and interactive features, and has led to many research advancements [19]. Tichon et al. [20-22] applied VR to miners in safety training and effectively improved their safety level. Kerridge, Kizil, and Bruzzone et al.[23-25] built a VR framework that can evaluate and analyze the underground risks of mining. Using a head mounted display (HMD) and other means of interaction, Foster Pet al.[26,27,30] conducted an training operation simulation for underground miners in an interactive and immersive environment, where the simulated continuous mining machine and drilling machine could be operated to train remotely. Stothard[28-29] designed a VR coal industry training simulator that allows miners to experience the consequences of decision-making errors and learn from their mistakes. Based on a computer VR simulator, Stothard[40] also developed a mining classification method, and simulated the process with a short example. Based on VR and AR technology, Zhang [31] obtained dynamic images that were a fusion of real images and a virtual scene of the fully mechanized coal mining face. These dynamic images had better results that were closer to reality. Based on

the complete simulation data, Akkoyun [32-33] established an interactive mining and engineering visualization environment for teaching that demonstrated an open pit of magnesite. Zhang et al. [34-35,38-39] established a series of virtual mining models that included shearer, scraper conveyor and hydraulic support, and simulated the entire kinematics process and technique of fully mechanized coal mining face. By using fuzzy logic, neural networks and the 3D finite element method, Torano [36] simulated the longwall mining roof behavior and realized the 3D display of the longwall mining face with VRML language. Sun [37] established a digital information shearer platform that simulated the shearer movements of coal cutting, the adjustments of roller height, and the rotation of drum. Wan et al. [43-45] also studied from the point of coal and rock caving, monitoring respectively. Li[41-42] built a simple GUI interactive interface to simulate the process of fully mechanized coalmining face. On the basis of these virtual simulations, virtual monitoring appeared gradually and combined with the actual parameters in real time[46-48].In regard to its application in the mining field, VR technology has already achieved many successful results.

As mentioned above, the VR simulations in the mining field focused on aspects including safety training, operation process simulation, kinematics simulation, and visualization of the underground scene. It has been used mainly in the training and teaching fields and does not have as much prevalence in the industrial field. Therefore, the application level of VR technology in the mining industry is still relatively low, as there is no real industrial application. VR planning has not yet been applied in the mining industry. The following five points illustrate the reasons that limit this development.

(1) Due to the static and simplex nature of the simulation parameters, complex and dynamic scenes include the effects from many various factors cannot be simulated within a single simulator;

(2) There is no mathematical model for supporting, as the existing simulators can show only the process;

(3) The datum in the simulation process cannot be exported, so the simulator cannot provide in-depth analysis and decision-making skills;

(4) There is some lacking analysis in the information interaction between equipment and equipment as well as the information interaction between equipment and the environment;

(5) The virtual simulation parameters do not correspond to real parameters;

Therefore, the existing mining virtual simulation leads to many defects and cannot provide support for industrial applications such as planning and design, scheme argumentation, decision support, and other aspects of comprehensive management.

In Industrial 4.0, SIEMENS first proposed the so-called digital win model, in which all elements in the actual production process are digitalized, and all involved production processes can be simulated and analyzed within this digital level. This model can predict the events that are likely to occur in the actual production process and help avoid unnecessary investment losses before production begins. However, the application of VR technology remains relatively rare in coal-mining equipment, and a large gap remains to be filled in genuinely promoting the development of coalmining equipment.

A fully mechanized coal-mining face is the most critical link in the coal industry. Therefore, based on the above analysis, this paper will establish a VR simulator that can solve the problem of the fully mechanized coalmining face and carry out visual planning details. This advancement will help with decision making in the conceptual design, design selection and actual operation stages of the mining project. After analyzing the application and development of fully mechanized coalmining equipment and VR technology in detail, a fully mechanized Unity3D simulator (FMUnitySim), which can plan and adjust the three machines' key parameters online, is proposed in terms of mathematics and artificial intelligence. The remainder of this paper is organized as follows. Section 2 introduces the overall framework of the system. Sections 3 and 4 illustrate the collaborative

mathematical model of three machines and collaborative planning model based on an MAS, respectively. Section 5 discusses the method and technology realization in Unity3D. The simulation system and parameter matching experiments are tested and analyzed in section 6. Section 7 concludes this study.

2. Framework of FMUnitySim

2.1 Overall framework

Based on the established collaborative mathematical model of three machines in a dynamic environment and the MAS theory, FMUnitySim (Fig. 1) defines the virtual behaviors of three machines and their interactions with the virtual environment using C# script in Unity3D, thereby enabling the visualization of the entire planning process and enabling all relevant process data to be acquired and analyzed.

Figure 1 to be inserted here.

2.2 Collaborative mathematical model of three machines

The entire coordination process of the three machines is in accordance with the shearer location and relevant regulations. The hydraulic supports in different areas will take diverse but coordinated actions: those in the front of the shearer flap out, whereas those at the rear of the shearer slide in front of the support, which constitutes the support of the suspended roof and coal wall after coal cutting. After the sliding advance of the support, the hydraulic supports will push the scraper conveyor close to the coal wall side and load the falling coal to be shipped out. The overall goal of coordinating these three machines is to (1) automatically move the coalmining equipment, (2) avoid any interference between the shearer and hydraulic support, (3) maintain and guarantee the suitable running posture and straightness of the scraper conveyor, (4) effectively manage the coal wall and roof of the coalmining face, and (5) ensure that the hydraulic support strength attain the initially specified value.

To achieve these goals, the three machines must work in close coordination and achieve effective interaction with the underground environment. Fig. 2 shows the influencing factors in the three machines for different geological conditions at the coalmining face.

(i) The coordinated operation of the three machines requires the ability of comprehensive organization, with which the information from the ever-changing underground environment, mutative equipment conditions, supplier devices, running speed of shearer, and scraper conveyor load can be accordingly synthesized, optimized, and controlled.

(ii) The coordinated operation of three machines requires adaptation and optimization capabilities with which the shearer haulage speed and numbers and parameters of the advancing mode can be automatically adjusted according to various production scenarios and roof conditions.

Figure 2 to be inserted here.

2.3 Collaborative planning model based on an MAS

As the core of multi-agent analysis, coordination and cooperation enable the knowledge, expectations, intentions, planning, and actions to collaborate with one another. In other words, the coordination in an MAS is a process in which all agents interact with one another to achieve a common goal in a compatible and harmonic manner and avoid deadlocks or mutual locks among the agents.

Therefore, in this study, the shearer, scraper conveyor, grouped hydraulic supports, hydraulic system and underground environment are taken as an agent; they swap and sense information with one another, which affects and controls their behaviors. The interactions among all agents of the three machines and the environment used to effectively cut and transport coal are shown in Fig. 3.

Figure 3 to be inserted here.

2.4 VR planning method

In the VR environment of Unity3D, virtual equipment can be controlled by a programmed C# script based on the collaborative mathematical model and collaborative planning model.

(1) With the control of CmjAgent.cs, the virtual shearer can realize coordinated motion between the rocker arm and vertical steering cylinders, control the shearer haulage speed and direction, and simulate the movement of the real shearer.

(2) With the control of GbjAgent.cs, the virtual scraper conveyor can be adaptively laid on the virtual floor with the ability to push itself to the coal wall side and virtually transport and detect the ship capacity of coal.

(3) With the control of YyzjAgent.cs, the hydraulic support can perform movement, such as setting the legs, retracting the legs, advancing the support, and pushing the conveyor.

(4) Under the control of YyxtAgent.cs, the hydraulic system can provide hydraulic oil for hydraulic supports according to different conditions.

(5) With the control of EnvAgent.cs, the virtual environment can construct the virtual roof and floor from XML data, which are assigned by the users, to stimulate the mine pressure and broken roof.

3. Collaborative mathematical model of the three machines

3.1 Coupling of the shearer haulage speed and scraper conveyor load

With differences in the shearer haulage speed and location, the scraper conveyor typically changes its chain speed to maintain its rated load. Therefore, an accurate coupling analysis must be conducted, and the shearer haulage speed must be calculated for the scraper conveyor load.

3.1.1 Instantaneous withstanding maximum load

The following research results can be obtained from reference [49]:

The maximum permitted coal transporting amount is calculated as

$$Q_{permit} = (0.83 * N_{motor} - \frac{2q_0 L v_g \cos\beta f_1}{102\eta}) \frac{102\eta}{v_g(\cos\beta \pm \sin\beta)} \quad (3.1)$$

For the SGZ768/630-type scraper conveyor, the sectional area to transport coal is calculated according to reference [49] as

A_{area}=0.48 m^2.

The amount of coal stream per meter in the middle trough is calculated as

$$A(t) = \begin{cases} \frac{Q(t)}{3.6K_g v_0} & \frac{Q(t)}{3.6K_g v_0} < A_{area} \\ A_{area} & \frac{Q(t)}{3.6K_g v_0} \geq A_{area} \end{cases} \quad (3.2)$$

3.1.2 Analysis of cutting with the coal-transporting process

For a shearer that cuts coal from its head to its tail, if the roof is assumed to be undulating and the floor is assumed to be flat, then the transporting coal process is as shown in Fig. 4.

Figure 4 to be inserted here.

The conversion conditions of four phases must satisfy the conditions shown in Table 1.

Table 1 to be inserted here.

3.1.3 Calculation of the coal cutting amount

We assume that a good coal-rock recognition device is installed in the shearer or that the operators can clearly distinguish the interface between coal and rock; then, the cutting amount of the front drum can be approximated as the full diameter of the front drum, and the cutting amount of the rear drum can be calculated according to the cutting trajectory of the front drum, as shown in Fig. 5.

Figure 5 to be inserted here.

As shown in Fig. 5, the definition of the coal seam curve is a series of feature points of cutting height per length of the middle trough in the X coordinates. Thus, the feature points of the cutting height of the rear drum are ($X(i)$, $H_u(i)$-D_{drum}).

Define $\lambda = (S_r(t)\text{-}S_r(t_3))/D_{zbc}$ and the remainder $\mu = (S_r(t)\text{-}S_r(t_3))\%D_{zbc}$.

Because the coal seam height changes slowly, the cutting line that connects two adjacent cutting points can be considered a straight line. Accordingly, the cutting area of two adjacent cutting points can be considered a trapezoid.

The coal cutting amount of the front drum and rear drum can be calculated as shown in Equations (3.3) and (3.4), respectively.

$$m_{front} = (S_f(t) - S_f(t_1) + L_y \cos\alpha_{t_1} - L_y \cos\alpha_t) * D_{drum} * J * \rho_{soild} \quad (3.3)$$

$$m_{rear} = (\sum_{i=1}^{\lambda-1}(h_u(i)+h_u(i+1)-2*D_{drum})*D_{zbc}/2 + (\frac{(h_u(\lambda+1)-h_u(\lambda))\sigma}{D_{zbc}}+2*(h_u(\lambda)-D_{drum}))*\sigma/2)*J*\rho_{\text{soild}} \quad (3.4)$$

The instantaneous coal cutting amount of the front and rear drums is calculated as shown in Equations (3.5) and (3.6) respectively.

$$m_{Ins-front}(t) = V_c * D_{drum} * J * \rho_{\text{soild}} \quad (3.5)$$

$$m_{Ins-rear}(t) = V_c * f(s_r(t)) * J * \rho_{\text{soild}} \quad (3.6)$$

The instantaneous amount of shipped coal is calculated as

$$m_{Ins-transport}(t) = q(t) * v_g * \rho_{\text{dispersion}} \quad (3.7)$$

The total amount of shipped coal from moment t_2 to moment t is calculated as

$$m_{total-transport} = \sum_{i=t_2}^{t} m_{Ins-transport}(i) \quad (3.8)$$

The instantaneous load of the scraper conveyor is calculated as

$$Q(t) = m_{front}(t) + m_{rear}(t) - m_{total-transport}(t) \le Q_{permit} \quad (3.9)$$

If $Q(t)$ reaches the maximum allowed value Q_{permit}, the scraper conveyor load at moment t must satisfy the following condition:

$$Q_{Ins}(t) = m_{Ins-front}(t) + m_{Ins-rear}(t) - m_{Ins-transport}(t) < 0 \quad (3.10)$$

3.1.4 Coupling of the scraper conveyor load with the underground environment

In the hydraulic support process, the coal wall may suddenly collapse depending on the shearer location and running speed.

Whether collapse occurs mainly depends on the follower distance and mining height, and the common regulation is as follows: a higher mining height and greater follower distance correspond to a higher probability of coal wall collapse.

If this phenomenon occurs, the scraper conveyor load will change suddenly.

After this phenomenon occurs, it will not occur again within 50 m.

In this paper, assuming a scope of 50 m, if the follower distance is greater than 10 times D_{zbc}, the probability of collapse is calculated as follows:

$$f(p) = \begin{cases} 1 & D_{follow} \ge 10 * D_{zbc} \\ 0 & D_{follow} < 10 * D_{zbc} \end{cases} \quad (3.11)$$

where D_{follow} is the follower distance. The mutation load of the scraper conveyor is calculated as

$$m_{sudd} = (-1)^{f(p)} * Random.Range(0.75,1) * 2.5\text{t} \quad (3.12)$$

Considering the sudden collapse of the coal wall, the instantaneous load of the scraper conveyor is calculated as

$$Q(t) = m_{front}(t) + m_{rear}(t) - m_{total-transport}(t) + m_{sudd} \le Q_{permit} \quad (3.13)$$

3.2 Coupling of the shearer haulage speed and adjustment of the front drum height with the underground environment

Facing an undulating virtual roof, the virtual shearer can adjust the height of the front drum and adaptively plan according to its capacity.

Whenever the shearer runs along the length of the middle trough, the shearer will acquire the next roof height in advance and make a comparison with the current drum height. The shearer decides which action to take next according to the comparison result and ability of the hydraulic system.

When the shearer is operating at moment t, the rotate angle of the front drum is calculated as

$$\alpha_{S(t)} = \arcsin(\frac{H_u(i) - H_c - D_{drum}/2}{L_y}) \quad (3.14)$$

Due to the control strategy of the shearer or detected error of the coal seam height, the front drum is likely higher than the interface between coal and rock, and the front drum begins to cut the rock. In an abnormal electric current condition, the virtual shearer must reduce the height of the front drum.

The decision condition to determine whether the current is abnormal is as follows:

$$L_y \sin\alpha_i + H_c + D_{drum}/2 > H_{ui} \quad (3.15)$$

3.3 Coupling of the following control of hydraulic supports and the shearer haulage speed

3.3.1 Matching the advancing mode

The most important factor of the three-machine coordination is the matching of shearer haulage speed V_c and hydraulic support advancing speed V_y.

If $V_c<V_y$, the hydraulic support can follow the shearer action in a sequential advancing mode, where the phenomena of support loss and inadequate advancing do not appear. Before the shearer location triggers the next group action, the current group has completed advancing the action.

If $2V_y>V_c>V_y$, the hydraulic support cannot regularly follow the shearer action in a sequential advancing mode and must switch to the cross-grouping advancing mode under the premise of a favorable roof condition. The hydraulic supports can continue running in order only by the cross-grouping advancing mode.

In the course of shearer running, the swarm hydraulic supports automatically switch the advancing mode according to the detected shearer haulage speed and follower distance in real time.

YiJiaFangShi, which is a static variable defined in FMUnitySim, is used to mark the current advancing mode. *N,* which is a static variable defined in FMUnitySim, is used to mark the number of hydraulic supports, which conduct advancing action. If the value of YiJiaFangShi is equal to one, the current advancing mode is the sequential advancing mode, and the value of *N* is unique. If the value of YiJiaFangShi is equal to two, the current advancing mode is the cross-grouping advancing mode, and N is a smaller number.

3.3.2 State mark of the hydraulic support using the finite-state machine

Hydraulic support has six states, which are denoted as 1-6, as shown in Table 2.

Table 2 to be inserted here.

The hydraulic support must detect the distance between its position and the position of the front drum or rear drum. If the distance satisfies the rules shown below, the hydraulic support will take the corresponding actions.

(1) Rule 1: if the distance from its position to the position of the rear drum is less than two times D_{zbc}, the hydraulic support begins to successively retract the columns, advance the support and rise the columns.

(2) Rule 2: if the distance from its position to the position of the rear drum is within 10-15 m, the hydraulic support begins pushing the conveyor.

(3) Rule 3: If the distance from its position to the position of the front drum is less than two times D_{zbc}, the hydraulic support begins to flap out.

3.3.3 Realization of the sequential advancing mode

If the value of YiJiaFangShi is equal to one, the current advancing mode is the sequential advancing mode. The conditional relation is as follows:

$$state(z)=\begin{cases}1 & S_{zj}(z)-S_f(t)>2*D_{zbc}\\ 2 & (S_r(t)-S_{zj}(z)>(2-6)*D_{zbc})\cap(state(z-1)=5)\\ 3 & (state(z)=2)\cap(H_u(z)-H_{zj}(z)\geq H_{down})\\ 4 & (state(z)=3)\cap(S_{tuiyi}(z)=J)\\ 5 & (state(z)=4)\cap(H_u(z)-H_{zj}(z)\leq 0)\\ 6 & (S_r(t)-S_{zj}(z)>(7-10)*D_{zbc})\cap(state(z)=5)\end{cases} \tag{3.16}$$

3.3.4 Realization of the cross-grouping advancing mode

If the value of YiJiaFangShi is equal to two, the current advancing mode is the cross-grouping advancing mode. Suppose that hydraulic supports No. *z* and No. *z+2* maintain the cross-grouping advancing mode; then, hydraulic support No. *z* is calculated as shown I Equation (16), and hydraulic support No. *z+2* must be synchronized with hydraulic support No. *z*. The conditional relation is shown below.

$$state(z+2)=\begin{cases}1 & S_{zj}(z)-S_f(t)>2*D_{zbc}\\ 2 & state(z)=2\\ 3 & (state(z)=3)\cap(H_u(z+2)-H_{zj}(z+2)\geq H_{down})\\ 4 & (state(z)=4)\cap(S_{tuiyi}(z+2)=J)\\ 5 & (state(z)=5)\cap(H_u(z+2)-H_{zj}(z+2)\leq 0)\\ 6 & (S_r(i)-S_{zj}(z)>(7-10)*D_{zbc})\cap(state(z+2)=5)\end{cases} \tag{3.17}$$

3.3.5 Switching of the advancing mode

If the follower distance is greater than 11 times D_{zbc}, the shearer must decelerate. While waiting for the previous hydraulic support to finish advancing, the advancing mode switches from the sequential advancing mode to the cross-grouping advancing mode.

If the follower distance is less than 3 times D_{zbc}, the shearer must accelerate. Similarly, under the premise of waiting for the previous hydraulic support to finish advancing, the advancing mode switches from the cross-grouping advancing mode to the

sequential advancing mode.

3.4 Coupling of the following control of hydraulic supports with the condition of the roof and floor

When the underground environment is in a good condition, the advancing action of hydraulic supports must match the difference of the shearer haulage speed and location, which follow rules 1-3 in section 3.3.2. For a working face with a broken roof, the advancing mode of the support with pressure is recommended to prevent the roof from falling. The column retracting speed for the working face with a large mine pressure is slower than that under normal conditions because the relieving the pressure requires a long period of time.

With the continuous operation of three machines, the action speed of the swarm hydraulic cylinders gradually decreases because of the filter plug or other problems, which makes the original control parameters unsuitable. These problems may occur at any time in any hydraulic support; thus, the action quality cannot be effectively controlled.

The action time of the advancing supports can be calculated as

$$t_{norm-move} = (n_{broken}) * (n_{press})(n_{hy} * n_{condition} * (\frac{H_{rise}}{S_{r-l}} + \frac{H_{down}}{S_{d-l}} + \frac{J}{S_{r-t}})) \tag{3.18}$$

The values of the operating parameters are shown in Table 3.

Table 3 to be inserted here.

3.5 Coupling of the shape of the scraper conveyor and advancing units of the hydraulic supports

When the shearer runs in the feeding process, the scraper convey will form an s-shaped bending section. When the shearer runs in the normal cutting process, the straightness of every middle trough must be detected in real time.

We assume that the roof is flat and that each hydraulic support maintains the normal attitude, i.e., it does not appear askew, and no inclination occurs in the support advancing process. Therefore, the s-shaped and straightness of the scraper conveyor depend on the elongation of the advancing units for the corresponding hydraulic supports.

3.6 Delay or data loss

In the process of interacting with other machines, each machine may encounter delay or data loss. The interaction of the three machines is as follows: the shearer occupies the lead position in the three-machine movement, and the scraper conveyor and group hydraulic supports are auxiliary.

The shearer may obtain the number of hydraulic supports, which delays advancing support and results in a greater distance at the empty top. The shearer may also obtain the scraper conveyor's single load overrun, which causes a short-time overrun of the scraper conveyor. Conversely, this effect decreases the efficiency of the coal mining process.

By obtaining the shearer's location in real time, the advancing action of a single hydraulic support is continuous. However, the hydraulic supports in front of the shearer may retract the supporting plate farther backward than is normal, which causes a risk of interference.

Those behind the shearer will struggle more than normal while advancing support. This widens the empty distance and increases the collapse risk of the roof coal wall.

The definition of the reliability of data transmission is the probability that the communication system does not appear data transmission delay or loss. In this paper, the value of this parameter is 95% .

4. Collaborative planning model based on an MAS

4.1 Model of the shearer agent

An agent model of the shearer is shown in Fig. 6. The perception and communication module is used to interact with other agents (Table 4); then, the logical information processing module is used to reason, decide and transfer results to the execution and control module (Table 5), which manipulates the virtual shearer to take specific actions.

Figure 6 to be inserted here.

Table 4 to be inserted here.

Table 5 to be inserted here.

Module of logical information processing of

the shearer

The shearer haulage speed should be coupled with the conditions of the roof, scraper conveyor and hydraulic supports.

Coupled with the hydraulic supports, the virtual shearer must take corresponding actions when is facing the minimum and maximum distance of empty roof.

Coupled with the scraper conveyor load, if the scraper conveyor load is greater than the permitted maximum load, the instantaneous cutting amount of coal is not greater than the instantaneous transport amount of shipped coal.

Coupled with the roof plate, if the coal-rock interface identification is regularly working, a shearer should be in the normal condition. In contrast, when abnormal turning of the virtual electric current of motors occurs, the shearer must decelerate and decrease the height of the front drum by adjusting the front lifting cylinder.

4.2 Model of the scraper conveyor agent

The scraper conveyor has two functions: the shape, as shown in section 3.5, and the load, as shown in section 3.1. The corresponding relationship between the perception task of the scraper conveyor and the perception variables of the virtual scraper conveyor is shown in Table 6, and the corresponding relationship between the control task of the scraper conveyor and the virtual control variable of the scraper conveyor (GbjAgent.cs) is shown in Table 7.

Table 6 to be inserted here.

Table 7 to be inserted here.

Logic information processing module of the scraper conveyor

If the scraper conveyor load is greater than the maximum permitting load, the instantaneous amount of coal cut by the front and rear drums and the instantaneous amount of shipped coal must be detected online. If the former is greater than the latter, the shearer haulage speed must decelerate.

4.3 Model of the hydraulic support agent

There are currently over 100 hydraulic supports in the actual underground working face. Each hydraulic support must communicate with other agents and have the appropriate behavior for the current underground environment, as shown in Fig. 7.

Figure 7 to be inserted here.

The corresponding relationship between the perception task of the hydraulic support and the perception variables of the virtual hydraulic support is shown in Table 8, and the corresponding relationship between the control task of the hydraulic support and the control variable of the virtual hydraulic support (YyzjAgent.cs) is shown in Table 9.

Table 8 to be inserted here.

Table 9 to be inserted here.

Logic information processing module of the hydraulic support

Hydraulic support (i) must detect the distance between its position and the front drum or rear drum. If the distance satisfies rules 1, 2 and 3, hydraulic support (i) performs the corresponding actions.

In the support advancing process, it is necessary to couple the roof trajectory, mine pressure, hydraulic system and surrounding hydraulic supports, as discussed in section 3.3.2. The action of pushing the conveyor and advancing the support must be coupled with the shape of the scraper conveyor.

4.4 Model of the hydraulic system agent

The hydraulic system is mainly affected by the action mode and amount of swarm hydraulic supports. The corresponding relationship between the perception task of the hydraulic system and the perception variables of the virtual hydraulic system is shown in Table 10, and the corresponding relationship between the control task of the hydraulic system and the virtual control variable of the hydraulic system (YyxtAgent.cs) is shown in Table 11.

Table 10 to be inserted here.

Table 11 to be inserted here.

4.5 Model of the underground environment agent

As shown in Fig. 8, the agent of the underground environment can simulate the change in the underground environment parameters because of the operation of the three machines and regular events in the underground environment, which include the

collapse of the coal wall and broken roof caused by the empty roof distance and periodic mine pressure in the geology condition.

Figure 8 to be inserted here.

The corresponding relationship between the perception task of the environment and the perception variables of the virtual environment is shown in Table 12, and the corresponding relationship between the control task of the environment and the virtual control variable of the environment (EnvAgent.cs) is shown in Table 13.

Table 12 to be inserted here.

Table 13 to be inserted here.

5. VR planning method

To visually observe the entire simulation state, Unity3D must be integrated with a collaborative planning model based on MAS theory. Several common issues must be addressed, as discussed below.

5.1 3D model of the three machines

According to the scene mapping and a full set of drawings, the 3D model of the three machines is obtained and repaired in the UG(Unigraphics NX). Considering the capacity and pressure of the software and hardware, the external dimensions should be precisely modeled, and the internal transmission structures are ignored, as shown in Fig. 9.

Figure 9 to be inserted here.

The 3D model is imported into 3DMAX in stl format and converted into fbx format, which can access Unity3D. In this manner, virtual models that are consistent with the physical model are established in Unity3D.

5.2 Model of the underground environment

The underground environment includes the intellectual input of various types of variables, such as the roof height, mine pressure and broken degree.

In this paper, to plan in a convenient manner, the floor is ideally flat, and the roof height is described with 100 points of the cutting height of the front drum, which are collected using the actual underground coal wall.

The mine pressure and broken conditions are generated in the virtual scene according to the setting result that the users input into the GUI module.

5.3 GUI interface

The GUT interface can set up different initial conditions by entering different planning parameters. It is mainly divided into six modules.

(1) The module of geological terrain parameters is a general overview of the underground geological environment, which includes the dip angle of the coal seam, degree of broken roof, and mine pressure regulation.

(2) The module of the roof and floor parameters is responsible for the roof and floor parameters, which determine the generation of the virtual roof and floor in FMUnitySim.

(3) The module of the coal cutting method and process parameters includes the selection of coal cutting methods and three rules between the shearer and hydraulic supports.

(4) The module of the shearer parameters contains the movement and performance parameters, such as the scope and acceleration of the shearer haulage speed, scope of the permitted follower distance, and virtual current of the motor.

(5) The module of the scraper conveyor parameters includes the movement and performance parameters, such as the scope of the chain speed, power of the motor, detection of straightness, and collapse probability of the coal wall.

(6) The module of the hydraulic support parameters and hydraulic system includes the movement and performance parameters, such as the total amount, pressure and form of the hydraulic system.

6. Experiment and discussion

The experimental planning conditions in this paper are set as follows:

(1) The roof is assumed to be undulating, and the floor is assumed to be flat.

(2) The planning process belongs to the coal cutting stage of the shearer from the scraper conveyor head to the scraper conveyor tail, and this stage is part

of the end beveling feeding bidirectional coal cutting method.

(3) The uploading point of the scraper conveyor is assumed to be in its head section, and the direction of coal transport is assumed to be from high to low.

6.1 Design of the simulation experiment

Unity3D can be released on a PC platform or Web platform.

First, after the PC platform program is run, the "end of the oblique cut feed two-way coal cutting process" is selected as the mining method. Second, the specific values of rules 1, 2 and 3 are set as 3, 7 and 2, respectively, and the scope of the safety follower distance is set as 2-8. Third, the matched parameters of the three machines are moderately set, such as the action parameters of the hydraulic support and scope of the shearer haulage speed. Finally, stable coal-rock is selected in the geological terrain parameters, where the cross-grouping advancing mode is permitted.

When the simulation begins, the virtual shearer takes the following series of actions: lifting the left drum, descending the right drum and running toward the scraper conveyor tail section.

Because V_c is greater than V_y, when the shearer location begins to trigger the advancing action of hydraulic support No. n as rule 1 in section 3.3.2, hydraulic support No. $n+1$ cannot begin to move until hydraulic support No. n completes its advancing action. When Vy<Vc<2Vy, the cross-grouping advancing mode is triggered. In this process, the hydraulic support catches up with the shearer quickly. The scene in that moment is illustrated in Fig. 10.

Figure 10 to be inserted here.

When the follower distance is greater than a certain limit, the shearer automatically begins to decelerate and the hydraulic support begins to catch up with the shearer until the follower distance is smaller than the safe follower distance. Simultaneously, V_c increases.

With the program running, the generation and transmission of an s-shaped bending section caused by the action of gradually pushing the conveyor can be easily observed, as shown in Fig. 11.

Figure 11 to be inserted here.

Figure 12 to be inserted here.

Fig. 12 shows the planning relationship among V_c, D_{follow} and $Q(t)$.

Point A: Along the running length of L_{wan}, the shearer begins to cut coal with the front drum. Meanwhile, V_c increases from 0 to 10.2 m/min, and the advancing action of hydraulic support No. 1 has been triggered.

Point B: V_c will approach 20 m/min, which is the maximum value that the users can preset.

Point C: at this moment, $Q(t)$ changes suddenly, which results in an increase of 2 tons. This change occurs because if D_{follow} is ten times greater than D_{zbc}, the coal wall suddenly collapses. Meanwhile, the advancing mode switches from sequential to cross-grouping.

Point D: When D_{follow} reaches the maximum, which is equivalent to 12.8 times D_{zbc}, the empty roof may fall. At this time, the shearer must rapidly decelerate to make the hydraulic support quickly advance and gradually catch up to the shearer.

Point E: $Q(t)$ appears to decrease, and V_c is 11.63 m/min, which precisely matches $Q_{Ins}(t)$. Simultaneously, D_{follow} is less than the minimum safe follower distance, whose value is 3 times D_{zbc}. Interference may occur between the shearer and hydraulic supports; thus, V_c increases again to match $Q(t)$. Before reaching a balance, the entire process has fluctuated five times.

Point F: V_c increases again until $Q(t)$ has reached the maximum load.

Point F-G: After $Q(t)$ reaches the maximum load, V_c slightly decreases again.

Point G –H: A similar process is performed.

Point H: $Q(t)$ fluctuates in a small range until it reaches a stable state, where the sum of $m_{Ins-front}(t)$ and $m_{Ins-rear}(t)$ is equivalent to $m_{Ins-transport}(t)$.

Fig. 13 shows the relationship among $m_{Ins-front}(t)$, $m_{Ins-rear}(t)$ and scraper $m_{Ins-transport}(t)$. First, the front drum begins to cut coal; then, the scraper conveyor transports the shipped coal. Finally, the rear drum begins to cut coal, which must be calculated using the trapezoidal method in section 3.1.3.

$m_{front}(t)$ and $m_{rear}(t)$ change with V_c, and

$q(t)$ remains constant. Finally, a stable state at which $m_{Ins-front}(t)$ and $m_{Ins-rear}(t)$ are equivalent to $m_{Ins-transport}(t)$ occurs.

Figure 13 to be inserted here.

6.2 Matching of the optimal parameter

Experiments were performed to determine the best matching parameter in different experimental schemes (Table 14), where key planning parameters, such as the shearer haulage speed, follower distance, and scraper conveyor load, were set in different conditions and combined.

Table 14 to be inserted here.

The optimal parameters were mainly determined by the indicator of the time-velocity, safety efficiency (average follower distance), and average quality of coal production.

According to the above scheme, experiments were performed 10 times in every condition, and the average results of each group are shown in Table 15.

Table 15 to be inserted here.

The simulation results show the following:

(1) Compared with group 1, group 2 indicates that when collapse of the coal wall is considered, the safety efficiency is decreased and the other properties remain largely unchanged;

(2) A comparison of groups 2-5 indicates that to match the advancing speed of the hydraulic support, if the maximum shearer haulage speed is greater than the matching speed, a greater maximum shearer haulage speed corresponds to a greater average shearer haulage speed, lower security efficiency and a greater scraper conveyor load.

However, when the maximum shearer haulage speed increases, the average shearer haulage speed does not increase significantly, but the safety factor increases considerably. Hence, the shearer haulage speed should be selected to match the advancing speed of the hydraulic support and should not be larger because the short-term efficiency increases.

The comparison of groups 5 and 6 indicates that the average shearer haulage speed and coal cutting efficiency decrease considerably when the maximum shearer haulage speed is smaller than the matching speed. Only the safety factor improves slightly; thus, the maximum shearer haulage speed should not be less than the matching speed of the advancing speed of the hydraulic support.

(3) A comparison of groups 2 and 7 shows that when the direction of coal transportation is reversed, the average shearer haulage speed decreases, and the corresponding safety factor improves considerably. Thus, in this condition, the shearer haulage speed should be appropriately improved.

7. Conclusion and prospects

From the AI and VR perspectives, a VR collaborative planning simulator with its method for three machines in a fully mechanized coalmining face is developed with Unity3D based on the collaborative mathematical model and MAS. The main conclusions of this study are as follows:

(1) The proposed FMUnitySim can expand the application field of VR technology, not merely in industrial teaching and training. In particular, the application of VR in a fully mechanized mine face is a novel attempt of this study. With this application, the entire production process can be controlled and examined at the early stage of the project, and the type of selection design can be integrated with technique planning.

(2) The proposed FMUnitySim can considerably improve the digital design level of fully mechanized mining equipment. The equipment can be used to control the relationship between the entire system and a given part, and the operation details and strategy can be planned. With this VR simulation, various problems can be predicted, modified and optimized, thus reducing costs and increasing efficiency.

(3) Diversity and specialization in the design project are achieved for different environments and user requirements. The proposed FMUnitySim can provide a clearly visualized plan of the operational status of three machines in a fully mechanized coalmining face. It can also simulate the dynamic supporting relationship, attitude and performance of the three machines in terms of different working conditions that the users require. In summary, it provides theoretical support for the automation,

intelligentization and unmanned management of three machines in a fully mechanized mining face.

(4) By providing a broad vision for intelligentization and unmanned management, the proposed FMUnitySim can digitize and virtualize the entire process of fully mechanized coal mining. Then, FMUnitySim can solve the existing problems in fully mechanized coalmining equipment from the global system perspective and can accurately predict the possible development of the coalmining process. FMUnitySim makes a technological preparation for the digital model based on the virtual working face and an authentic image of the working face based on automation technology.

In this study, there are many complex constraints between the underground environment and the three machines, which consist of many unknown possible events. It is difficult to express the mathematical formula for so many unknown factors. Therefore, the collaborative mathematical model needs to further describe the complex underground environment.

In addition, this study simulated only the fully mechanized coalmining face, which is part of the mining industry. In the future, this industry could also apply the VR planning technique to other production aspects of the mining industry, such as digging, belt transportation, and mine hoisting. This paper has provided the theoretical support and technical support to advance the mining industry with new technology and information.

Future work will focus on integrating and incorporating FMUnitySim into the actual control system of the three machines to improve the efficiency. Future research goals include establishing an online planning system by reading the real-time information sensed from the three machines and better controlling the running of the three machines.

References

1. Wang, J.H.; Wang, Y.H.; Fu, J.H.: Crucial technology research and demonstration of digital mines. J China Coal Soc.**41**(6), 1323-1331 (2016)
2. Ge,S.R.: Key Technology of Intelligent Coal Mining Equipment. Coal Sci. Techno. **42**(9),7-11 (2014)
3. Niu, J.F.: Key Study on automatic and intelligent following control system of hydraulic powered support in fully-mechanized coal mining face. Coal Sci. Techno. **43**(12), 85-91(2015)
4. Wang, C.; Tu, S.; Chen, M.: Optimal Selection of a Longwall Mining Method for a Thin Coal Seam Working Face. Arab J. Sci. Eng. **41**(9),1-11 (2016)
5. Wang, J.H.; Huang, L.T.; Li, S.B.: Development of intelligent technology and equipment in fully-mechanized coal mining face, J China Coal Soc. **39**(8),1418-1423 (2014).
6. Fan, Q.G.; Li, Wei.: Study on Equipment Positioning and Task Coordination for Three Machines Controlling on the Mechanized Mining Face. China J. Mech. Eng. 9, 73-73 (2015)
7. Opensim, J.: A 3D Simulator for autonomous robots. http://opensimulator.sourceforge.net/ (2008). Accessed 14, April 2017
8. Freese, M.; Singh, S.; Ozaki, F.: Virtual robot experimentation platform v-rep: a versatile 3D robot simulator. In Simulation, Modeling, and Programming for Autonomous Robots, pp.51–62. Springer, Berlin Heidelberg (2010)
9. Mcdowell, P.; Darken, R.; Sullivan, J.: Delta3D: A Complete Open Source Game and Simulation Engine for Building Military Training Systems. J. Defense Model. Simulat. **3**(3),143-154 (2006)
10. Lewis, M.; Wang, J.; Hughes, S.: USARSim: Simulation for the study of human-robot interaction. J. Cognitive Eng. Decis. Making, **1**(1), 98–120 (2007)
11. Koenig, N.; Howard, A.: Design and use paradigms for gazebo, an open-source multi-robot simulator. In IEEE/RSJ International Conference on Intelligent Robots and Systems,28 September -2,October, no.3: 2149–2154.Sendai (2004)
12. Lee, W.; Cho, S.; Chu, P.: Automatic agent generation for IoT-based smart house simulator. Neurocomputing, **209**, 14–24 (2016).
13. Becker-Asano.; Christian.: A Multi-agent System based on Unity 4 for Virtual Perception and Wayfinding. Transportation Res. Procedia. 2:452-455 (2014)
14. Meng, Wei.; ROSUnitySim: Development and Experimentation of a Real-time Simulator for Multi-UAV Local Planning. Simulat. **92**(10), 002562-002567 (2016)
15. Meng, Wei.: ROS+unity: An efficient high-fidelity 3D multi-UAV navigation and control simulator in GPS-denied environments. Conference of the IEEE Industrial Electronics Society IEEE, 002562-002567 (2015)

16. Xu, Z.; Lu, X.Z.; Guan, H.: A virtual reality based fire training simulator with smoke hazard assessment capacity. Adv Eng. Softw.**68**(2),1-8 (2014)
17. Cha, M.; Han, S.; Lee, J.: A virtual reality based fire training simulator integrated with fire dynamics data. Fire Safety J. **50**(3),12–24 (2012)
18. Manca, D.; Brambilla, S.; Colombo, S.: Bridging between Virtual Reality and accident simulation for training of process-industry operators. Adv. Eng. Softw. **55**(1),1-9 (2013)
19. Kizil, M.S.: Virtual reality applications in Australian minerals industry. J. S. Afr. I. Min. Metall. **31**, 569-574 (2013)
20. Tichon, J.; Burgess,limerick. R.: A review of Virtual Reality as a medium for safety related training in Mining. J. Health Safety Res. Pract. **3**(1),33-40 (2011)
21. Perez, P.; Pedram, S.; Dowcet, B.: Impact of virtual training on safety and productivity in the mining industry. Conference: MODSIM 2013, Adelaid (2013)
22. Pedram, S.; Perez, P.; Dowsett, B.: Assessing The Impact Of Virtual Reality-Based Training On Health And Safety Issues In The Mining Industry. ISNGI2013 - International Symposium for Next Generation Infrastructure. (2013)
23. Pedram, S.; Perez, P; Palmisano, S.: Evaluating the influence of virtual reality-based training on workers' competencies in the mining industry. In A. G. Bruzzone, F. De Felice, M. Massei, Y. Merkuryev, A. Solis & G. Zacharewicz (Eds.), 13th International Conference on Modeling and Applied Simulation, MAS 2014 (pp. 60-64). Red Hook, New York, United States: Curran (2014).
24. Pedram, S., Perez, P.; Palmisano, S.: Evaluating 360-Virtual Reality for Mining Industry's Safety Training, International Conference on Human-Computer Interaction. Springer, Cham, pp.555-561 (2017)
25. Kerridge, A.P.; Kizil, M.S.; Howarth, D.F.: Use of virtual reality in mining education. The AusIMM Young Leader's Conference. The Australasian Institute of Mining and Metallurgy, pp.1-5 (2003)
26. Grabowski, A.: Jankowski, J.: Virtual Reality-based pilot training for underground coal miners. J. Safety Sci.**72**,310-314 (2015)
27. Foster, P.; Burton, A.: Virtual reality in improving mining ergonomics. J. S. Afr. I. Min. Metall. **104**(2), 129-133 (2004)
28. Stothard, P.; Laurence, D.: Application of a large-screen immersive visualization system to demonstrate sustainable mining practices principles. Trans. I. Min Metall. **23**,199-206 (2014)
29. Stothard, P.: The feasibility of applying virtual reality simulation to the coal mining operations. Australas. I Min. Metall. Publ. Ser. **5**,175-183 (2003)
30. Foster, P.J., Burton, A.: Modelling potential sightline improvements to underground mining vehicles using virtual reality. Trans. I. Min. Metall.**115**,85-90 (2013)
31. Zhang, S.X.: Augmented Reality on Longwall Face for Unmanned Mining. Appl. Mech. Materials. **40**-**41**(6), 388-391(2010)
32. Akkoyun, O.; Careddu, N.: Mine simulation for educational purposes: A case study. Comput. Appl. Eng. Educ.**23**(2),286-293 (2015)
33. Kijonka, M.; Kodym, O.; Coal industry technologies simulation with virtual reality utilization. Proceedings of the 13th International Carpathian Control Conference (ICCC), High Tatras, IEEE, 278-283 (2012)
34. Zhang, X.; An, W.; Li, J.: Design and Application of Virtual Reality System in Fully Mechanized Mining Face. Procedia Eng. **26**(4),2165-2172 (2011)
35. Wan, L.R.; Gao, L.; Liu, Z.H.: The Application of Virtual Reality Technology in Mechanized Mining Face. Adv. Intell. Syst. Comput. **181**,1055-1061 (2013)
36. Torano, J.; Diego, I.; Menéndez, M.: A finite element method (FEM) – Fuzzy logic (Soft Computing) – virtual reality model approach in a coalface longwall mining simulation. Automat. Constr. **17**(4),413-424(2008)
37. Sun, H.B.; Tan, C.; Yao, X.G.: Research on Three-Dimension Scene Modeling Technology of 3DVR Platform for Shearer. J. China Univ. Min. Technol. **39**(5), 676-681 (2010)

38. Xie, J.C.; Yang, Z.J.; Wang, X.W.: Design and Key Technologies of Virtual Assembly and Simulation of Mining, Driving and Transporting Equipment System. J. Syst. Simulat. **27**(4), 794-802 (2015)
39. Li, A.L.; Zheng, X.W.; Wang, W.: Virtual Motion Simulation of Hydraulic Support Based on Unity 3D.First International Conference on Information Sciences, Machinery, Materials and Energy. Atlantis Press (2015)
40. Stothard, P.; Squelch, A.; Stone, R.: Taxonomy of interactive computer-based visualization systems and content for the mining industry – part 2. International Future Mining Conference and Exhibition. OAI, vol.124, no.2, 201-210 (2015)
41. Li, W.N.: Fully Mechanized Three-Machine Linkage Process Simulation Based on Virtual Reality Technology. Dissertation Xi`an：Xi`an University of Science and Technology (2014)
42. Xu, X.Z.; Meng, X.R.; He, Y.R.: Research on virtual simulation of full mechanized mining face production based on three-dimensional visualization and virtual simulation. J. Safety Sci. Technol. 1,26-32 (2014)
43. Wan, L.R.; Gao, L.; Liu, Z.H.: The Application of Virtual Reality Technology in Mechanized Mining Face. Adv. Intell. Syst. Comput. **181**,1055-1061 (2013)
44. Tang S S, Wei C K. Design of Monitoring System for Hydraulic Support Based on LabVIEW. J. Adv. Mater. Res. **989-994**, 2758-2760 (2014)
45. Lo, J.Z.; Chen, H.Z.; Sui, G.: Study on Simulation System of Fully Mechanized Mining Face Based on Virtual Reality. J. Syst. Simula. **19**(18),4164-4167 (2007)
46. Li, H.; Chen, K.; Zhang, X.: Disign of monitoring and control system based on virtual reality technology on fully-mechanized coal mining face, Ind. Min. Autom. **42**(4),15-18 (2016)
47. Liang, S.; Chen, Y.; Zheng, X.: Study of monitoring system of hydraulic support movement state based on virtual reality. International Conference on Mechatronic Sciences, Electric Engineering and Computer. pp.3434-3437 (2013)
48. Yan, H.F.; Su, F.X.; Chen, Z.H.; A study on the remote monitoring system of hydraulic support based on 3DVR. Audio Language and Image Processing (ICALIP), 2010 International Conference on. IEEE, pp.912-915 (2010)
49. Wand, Y.: Design Manual for continuous conveying machinery. Beijing: China Railway Publishing House (2001)

Figures

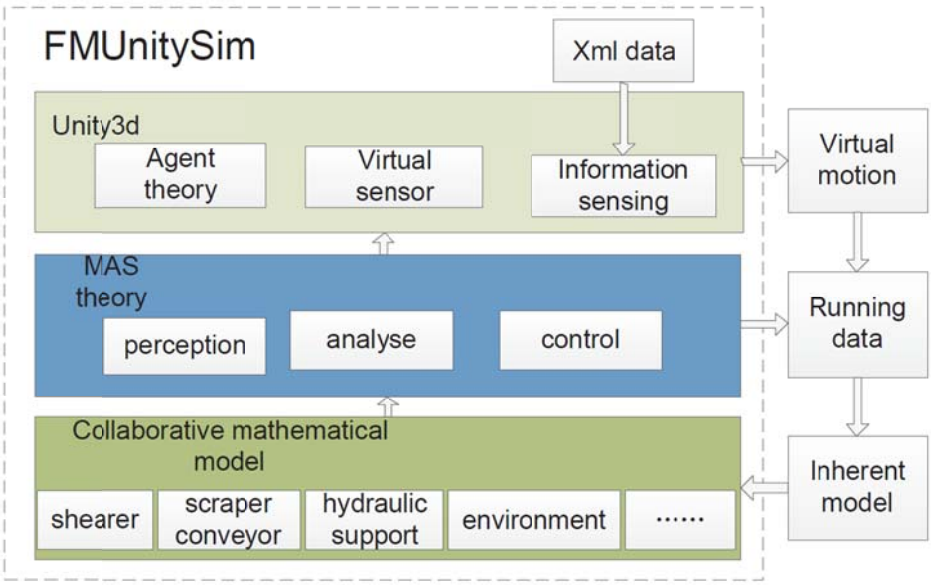

Fig. 1 Overall framework of FMUnitySim

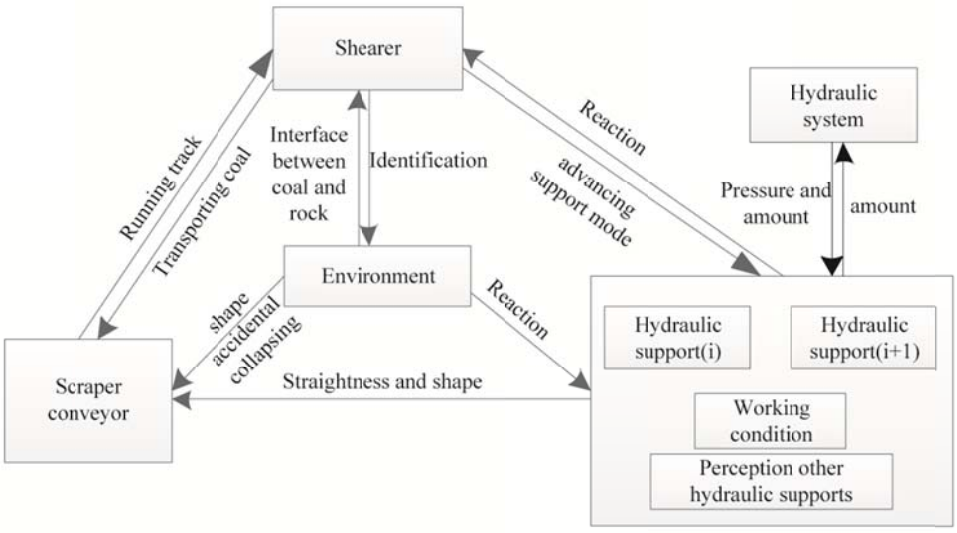

Fig. 2. Influencing factors for three-machine coordination with the external environment

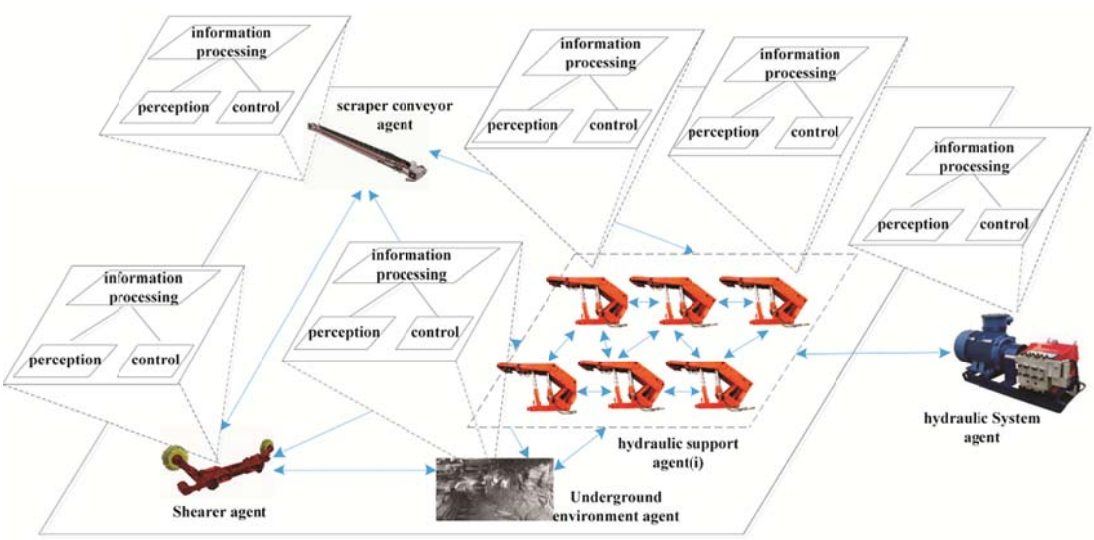

Fig. 3 Interaction among the agents of three machines and the underground environment

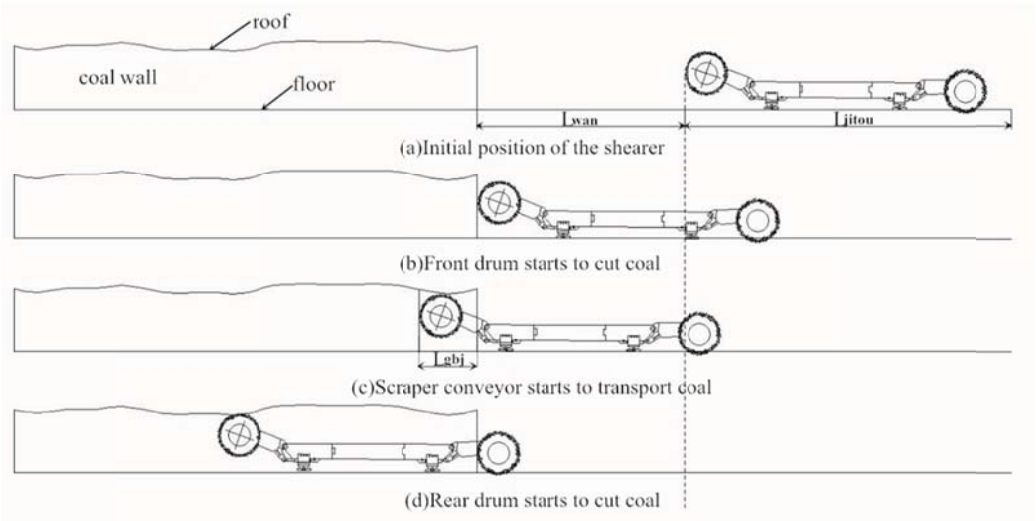

Fig. 4 **T**ransport process analysis

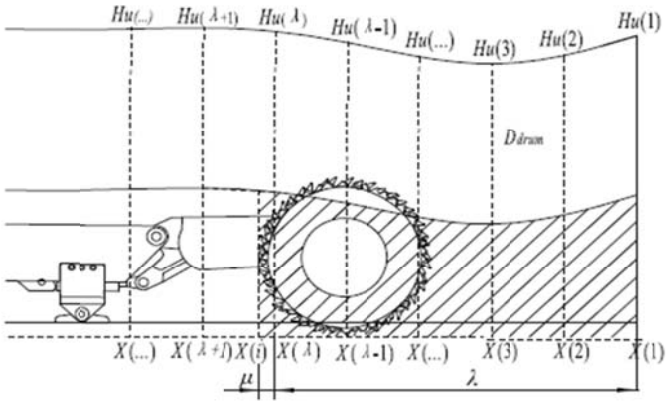

Fig. 5 Cutting curve of the rear drum

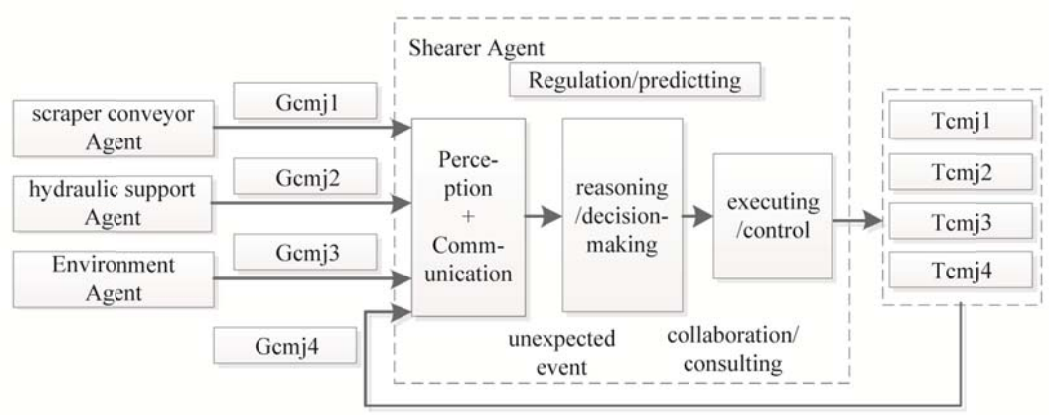

Fig. 6 Agent model of a shearer

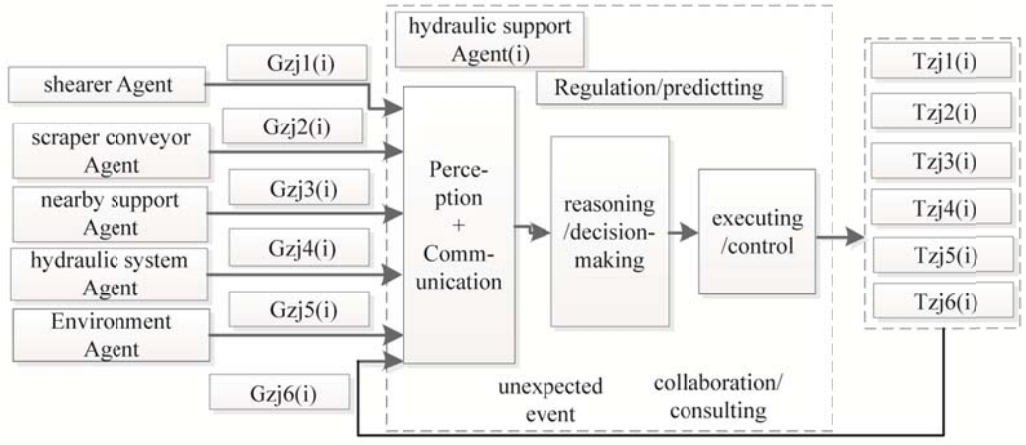

Fig. 7. Agent model of the hydraulic support

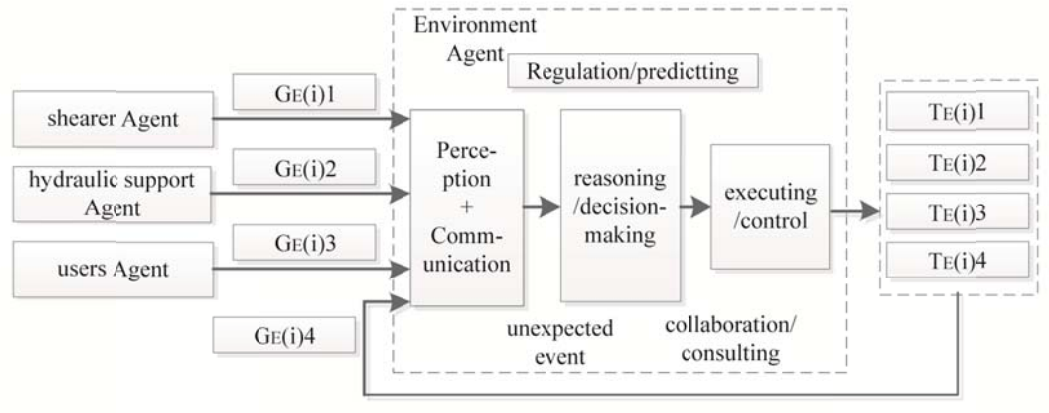

Fig. 8 Agent model of the environment

Fig. 9 Model repair results

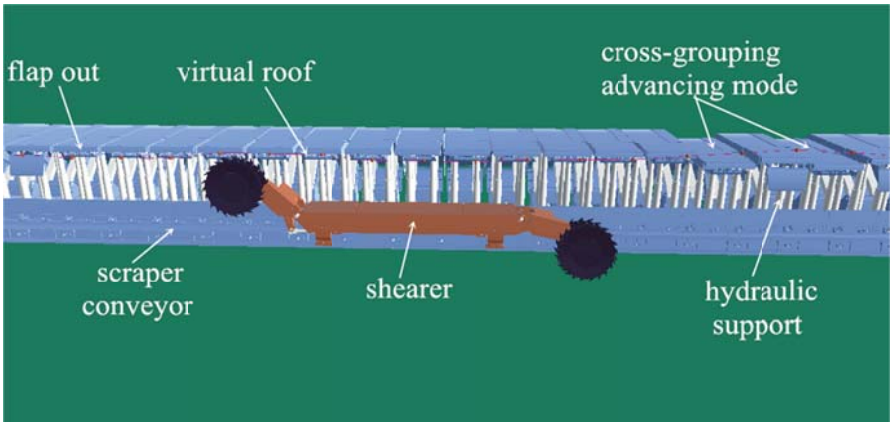

Fig. 10 Mutual perception between the shearer and hydraulic support

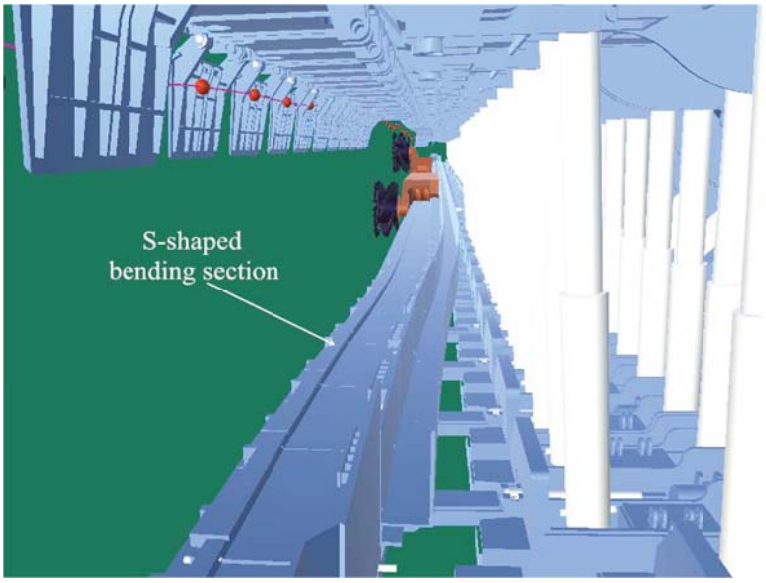

Fig. 11 S-shaped bending section

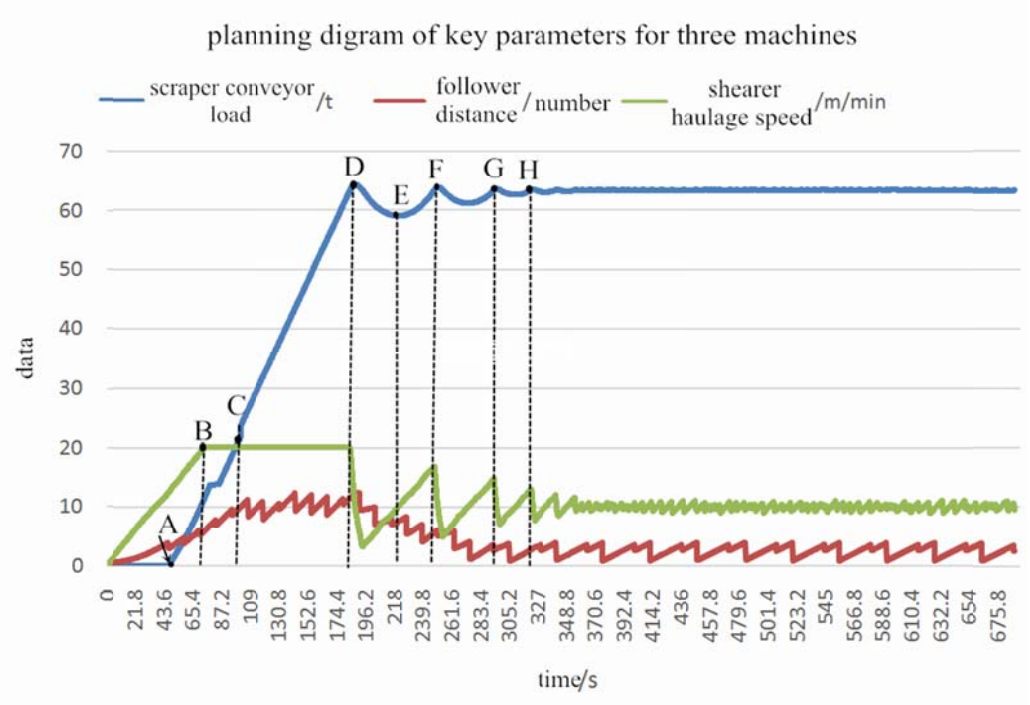

Fig. 12 Planning relationship among Shearer haulage speed, Follower distance and Total load of the scraper conveyor from the beginning to moment t

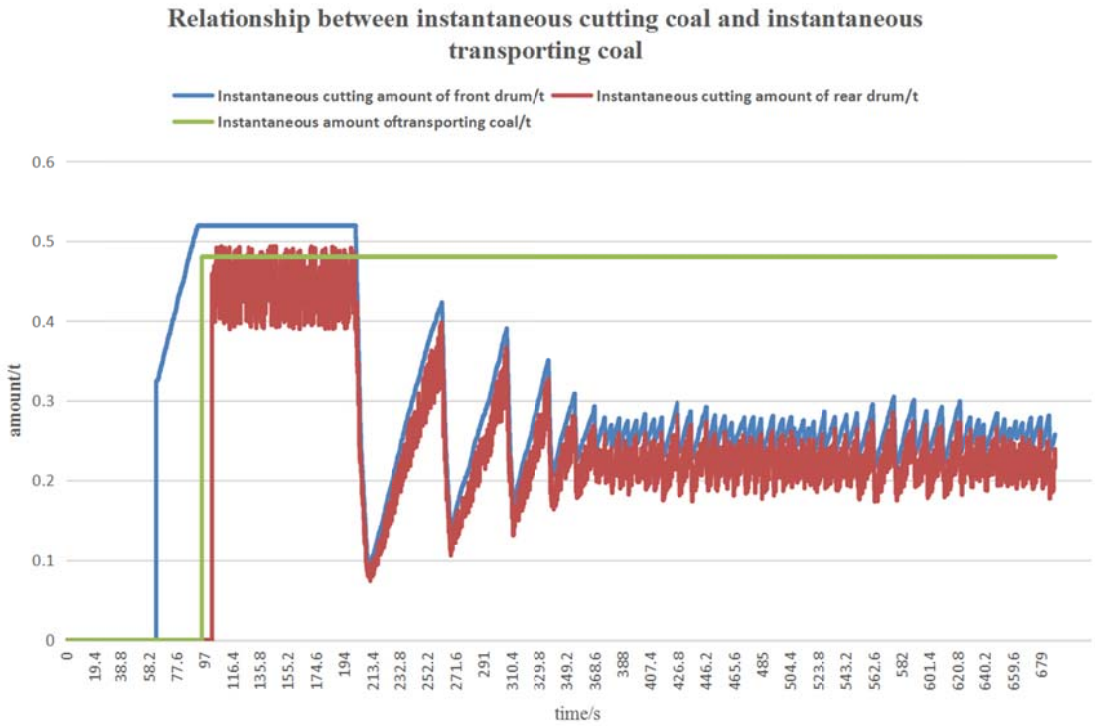

Fig. 13 Relationship among Cutting amount of the front drum from the beginning to moment t Coal cutting amount of the rear drum from the beginning to moment t

Tables

Table 1 Conversion conditions for the four stages

Transformation Stage	Conditions
(a)->(b)	$S_f(t_1) - S_f(t_0) + (L_y \cos\alpha_{S(t_1)} - L_y \cos\alpha_{S(t_0)}) > L_{wan}$
(b)->(c)	$\begin{cases} S_f(t_2) - S_f(t_1) + (L_y \cos\alpha_{S(t_2)} - L_y \cos\alpha_{S(t_1)}) = L_{gbj} \\ \int_{t_2}^{t_1} V_g dt = L_{wan} + L_{jitou} \end{cases}$
(c)->(d)	$S_r(t_3) - S_r(t_0) > L_{wan} + L_{JiShen} + L_y \cos\alpha_{S(t_0)} + D_{drum}/2$

Table 2 Corresponding state numbers of the hydraulic support

State	Flapping out	Retracting columns	Advancing support	Rising columns	Flapping in	Pushing conveyor
Number	1	2	3	4	5	6

Table 3 Values of the operating parameters

Operating Parameters	Value	Conditions
n_{broken}	1.5-2.0	$B_{zj}(i) \geq B_{normal}$
	1	$B_{zj}(i) < B_{normal}$
n_{press}	1.3-1.5	$P_{zj}(i) \geq P_{normal}$
	1	$P_{zj}(i) < P_{normal}$
n_{hy}	1-1.1	$YiJiaFangShi = 1$
	1.3-1.5	$YiJiaFangShi = 2$
$n_{condition}$	1-1.15	The value is larger for a longer running time.

Table 4 Relationship between the perception task of the shearer and the perception variables of the virtual shearer

ID	Perception task of the shearer	Perception variables of the virtual shearer
1	Gcmj1: coal-rock interface identification. Acquire the height and properties of the roof point located at the front of the former drum.	$H_u(i)$
2	Gcmj2: determine the load state of the scraper conveyor	$Q(t)$, $Q_{lns}(t)$
3	Gcmj3: determine the state of the swarm hydraulic supports and empty roof	N, D_{follow}
4	Gcmj4: determine the state of itself. An abnormal motor is determined based on the fail rate of coal-rock interface identification	I_{motor}

Table 5 Relationship between the control task of the shearer and the control variables of the virtual shearer

ID	Control task of the shearer	Control variables of the shearer
1	Tcmj1: control the front lifting cylinder	$\alpha_{S(t)}$
2	Tcmj2: control the rear lifting cylinder	$\alpha_{rS(t)}$
3	Tcmj3: control the shearer haulage speed	V_c
4	Tcmj4: control the updating motion track	$S_{tuiyi}(1), \ldots, S_{tuiyi}(m), \ldots S_{tuiyi}(m_{\max})$
5	Tcmj4: control the virtual current	I_{motor}, $\alpha_{S(t)}$

Table 6 Corresponding relationship between the perception task of the scraper conveyor and the perception variables of the virtual scraper conveyor

ID	Perception task of the scraper conveyor	Perception variables of the virtual scraper conveyor
1	Ggbj1: determine the load state of the scraper conveyor	$Q(t)$, Q_{Ins}
2	Ggbj(i)2: determine the attitude and shape of the middle troughs	$S_{tuiyi}(i-1)$, $S_{tuiyi}(i)$, $S_{tuiyi}(i+1)$

Table 7 Corresponding relationship between the control task of the scraper conveyor and the control variables of the virtual scraper conveyor

ID	Control task of the scraper conveyor	Control variable of the scraper conveyor
1	Tgbj1: control the chain speed	V_g

Table 8 Corresponding relationship between the perception task of the hydraulic support and the perception variables of the virtual hydraulic support

ID	Perception task of the hydraulic support	Perception variables of the virtual hydraulic support
1	Gzj(i)1: determine the parameters of the virtual shearer (location, attitude, and haulage speed)	$S_f(i)$, $S_r(i)$, V_c
2	Gzj(i)2: determine the control of the fixed range of middle trough No. *i* (attitude and shape)	$S_{tuiyi}(i)$
3	Gzj(i)3: determine the control of the hydraulic support for a fixed range of No. *i* (inclined and straight)	*YiJiaFangShi*
4	Gzj(i)4: determine the flow and amount of the hydraulic system	n_{hy}, *YiJiaFangShi*
5	Gzj(i)5: determine the condition of the underground environment	$B_{zj}(i)$, $P_{zj}(i)$, n_{broken}, $n_{pressure}$
6	Gzj(i)6: determine the state of itself	$n_{condition}$

Table 9 Corresponding relationship between the control task of the hydraulic support and the control variables of the virtual hydraulic support

ID	Control task of the hydraulic support	Control variables of the virtual hydraulic support
1	Tzj(i)1: control task of flapping out; State=1	$\phi(i)$
2	Tzj(i)2: control task of retracting columns; State=2	$H_{zj}(i)$
3	Tzj(i)3: control task of advancing support; State=3	$S_{tuiyi}(i)$
4	Tzj(i)4: control task of rising columns, State=4	$H_{zj}(i)$
5	Tzj(i)5: control task of flapping in; State=5	$\phi(i)$
6	Tzj(i)6: control task of pushing conveyor; State=0	$S_{tuiyi}(i)$

Table 10 Corresponding relationship between the perception task of the hydraulic system and the perception variables of the virtual hydraulic system

ID	Perception task of the hydraulic system	Perception variables of the virtual hydraulic system
1	Grb1: determine the action mode and amount of swarm hydraulic supports	*YiJiaFangShi*

Table 11 Corresponding relationship between the control task of the hydraulic system and the control variables of the virtual hydraulic system

ID	Control task of the hydraulic system	Control variables of the virtual hydraulic system
1	Trb1: control the flow	n_{hy}
2	Trb2: control the pressure	n_{press}

Table 12 Corresponding relationship between the perception task of the environment and the perception variables of the virtual environment

ID	Perception task of the environment	Perception variables of the virtual environment
1	G_E(i)1: determine the empty roof distance	$S_r(i)$-$S_{zj}(N)$
2	G_E (i)2: determine the roof effect from the hydraulic supports	$H_u(i) - H_{zj}(i)$
3	G_E (i)3: determine the periodic mine pressure	$B_{zj}(i)$, $P_{zj}(i)$, n_{broken}, $n_{pressure}$
4	G_E (i)4: determine the initial input by users	$H_u(i)$

Table 13 Corresponding relationship between the control task of the environment and the control variables of the virtual environment

ID	Control task of the environment	Control variables of the virtual environment
1	$M_E(i)1$: control the mine pressure	*YiJiaFangShi*
2	$M_E(i)2$: control the broken roof	$P_{zj}(i)$, n_{press}
3	$M_E(i)3$: control the collapsing of the coal wall	m_{sudd}
4	$M_E(i)4$: control the users' input information	$H_u(m)$

Table 14 Design of the experimental scheme

ID	Setting conditions of the simulation (only changing a single variable while keeping the other parameters constant)(the reliability of data transmission is set to 95%)
1	No consideration of the collapse of the coal wall, and the maximum shearer haulage speed is set to 20 m/min.
2	Consideration of the collapse of the coal wall, and the maximum shearer haulage speed is set to 20 m/min.
3	Consideration of the collapse of the coal wall, and the maximum shearer haulage speed is set to 17 m/min.
4	Consideration of the collapse of the coal wall, and the maximum shearer haulage speed is set to 15 m/min.
5	Consideration of the collapse of the coal wall, and the maximum shearer haulage speed is set to 12.5 m/min.
6	Consideration of the collapse of the coal wall, and the maximum shearer haulage speed is set to 10 m/min.
7	Consideration of the collapse of the coal wall, the maximum shearer haulage speed is set to 20 m/min and the direction of transporting coal is reverse.

Table 15 Experimental results

ID	Time-velocity (m/min)	Safety efficiency (average follower distance) (width)	Maximum empty roof distance(width)	Average quality of coal production (t)
1	11.49	4.87	13.31	51.79
2	11.45	4.95	13.85	51.85
3	11.53	4.74	11.76	50.03
4	11.59	3.65	10.24	46.49
5	11.71	3.47	9.03	35.27
6	9.57	3.28	8.17	21.47
7	11.14	4.29	13.01	51.19